Can we use zero density potentials in the semidilute regime?

- for $\rho/\rho^* \leq 1$ polymer do not overlap and the polymer-polymer effective potential is density independent
- for $\rho/\rho^* > 1$ polymer starts to overlap and the effective potential by HNC is state dependent

- Multi-blob representation:

  divide a long polymer of *N* monomers in *n* effective segments each grouping *l*=*N*/*n* monomers

  segment radius of gyration $r_g \sim bl^\nu$

  segment-segment overlapping density: $\rho_s^* = \dfrac{3}{4\pi r_g^3} = \rho^* n^{3\nu}$

  segment-segment effective interactions are density independent if

$$1 \geq \rho_s/\rho_s^* = (\rho/\rho^*)n^{1-3\nu} \Longrightarrow \rho/\rho^* < n^{3\nu-1} = n^{0.77}$$

By increasing the number of segments per chain we can safely use density independent potentials.

THE JOURNAL OF CHEMICAL PHYSICS **127**, 171102 (2007)

A soft effective segment representation of semidilute polymer solutions

Carlo Pierleoni
INFM CRS-SOFT, University of L'Aquila, I-67010 L'Aquila, Italy
and Physics Department, University of L'Aquila, I-67010 L'Aquila, Italy

Barbara Capone[a)] and Jean-Pierre Hansen
University Chemical Laboratory, Lensfield Road, Cambridge CB2 1EW, United Kingdom

Effective segment representation

- Potentials between two equal halfs of a single chain from MC:

$$v_{ss}(r)/k_BT = Ae^{-\alpha(r/r_g)^2}$$

$$\phi_b(r) = v_{ss} + \frac{k}{2}(r - r_0)^2 + const$$

- Transferability assumption: use $v_{ss}(r/r_g)$ between any non adjacent pair of segments in the multi chains case.

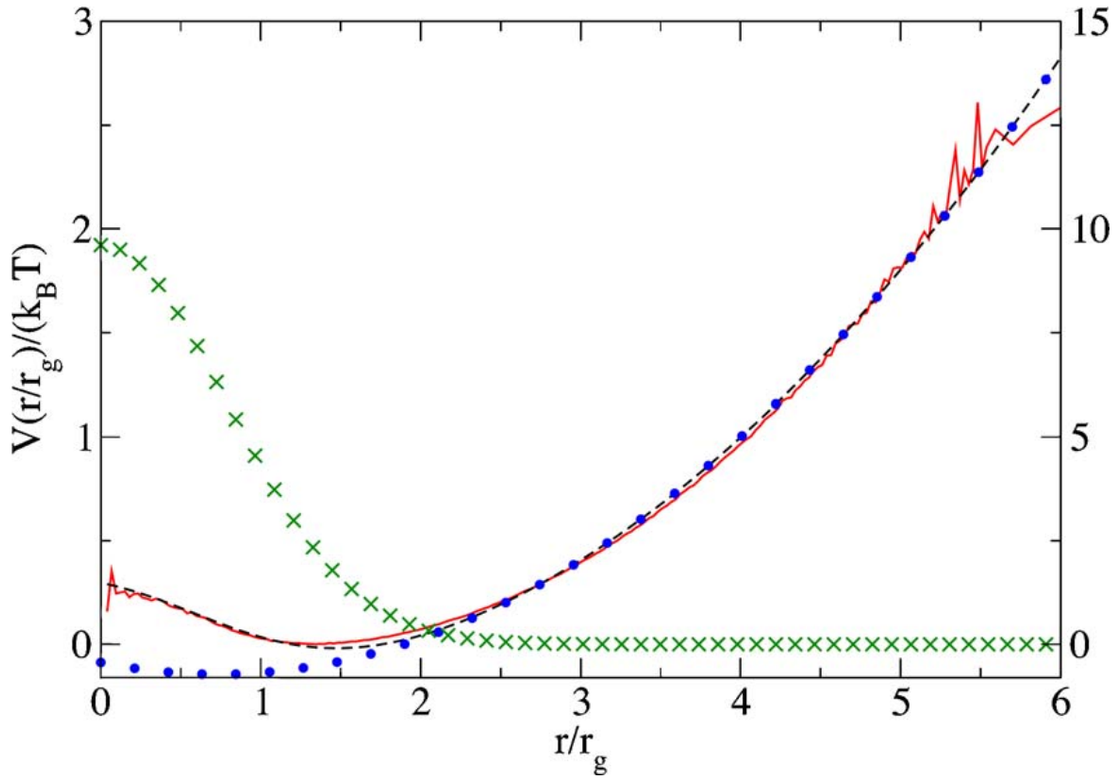

FIG. 1. (Color online) Effective potentials $\phi(r)$ between bonded (right-hand scale, continuous line) and $v(r)$ between nonbonded (left-hand scale, crosses) effective segments in units of k_BT, as computed by MC simulations of an $L=2000$ SAW polymer, divided into two equal segments. $v(r)$ is accurately fitted by the Gaussian [Eq. (1)] with $A=1.92$ and $\alpha=0.80$. $\phi(r)$ is represented by the form [Eq. (2)] (dashed curve) with the harmonic tethering potential fitted by $0.534(r/r_g-0.730)^2-0.724$ (dots).

The higher the density, the larger the number of segments, the smaller their radius of gyration, the steeper the potential.

In the limit n=M, we go back to the full monomer representation (not gaussian though).

Effective segment representation

$$S(k) = \frac{1}{Nn^2}\langle \rho_{\mathbf{k}} \rho_{-\mathbf{k}} \rangle = S_{\text{intra}}(k) + \frac{1}{n^2} \sum_{\alpha} \sum_{\beta} s_{\alpha\beta}(k),$$

where

$$\rho_{\mathbf{k}} = \sum_{i=1}^{N} \sum_{\alpha=1}^{n} \exp(i\mathbf{k} \cdot \mathbf{r}_{i\alpha})$$

The scaling exponent is independent on the chosen resolution

$$S(k) \sim k^{-1/\nu} \qquad kR_g >> 1$$

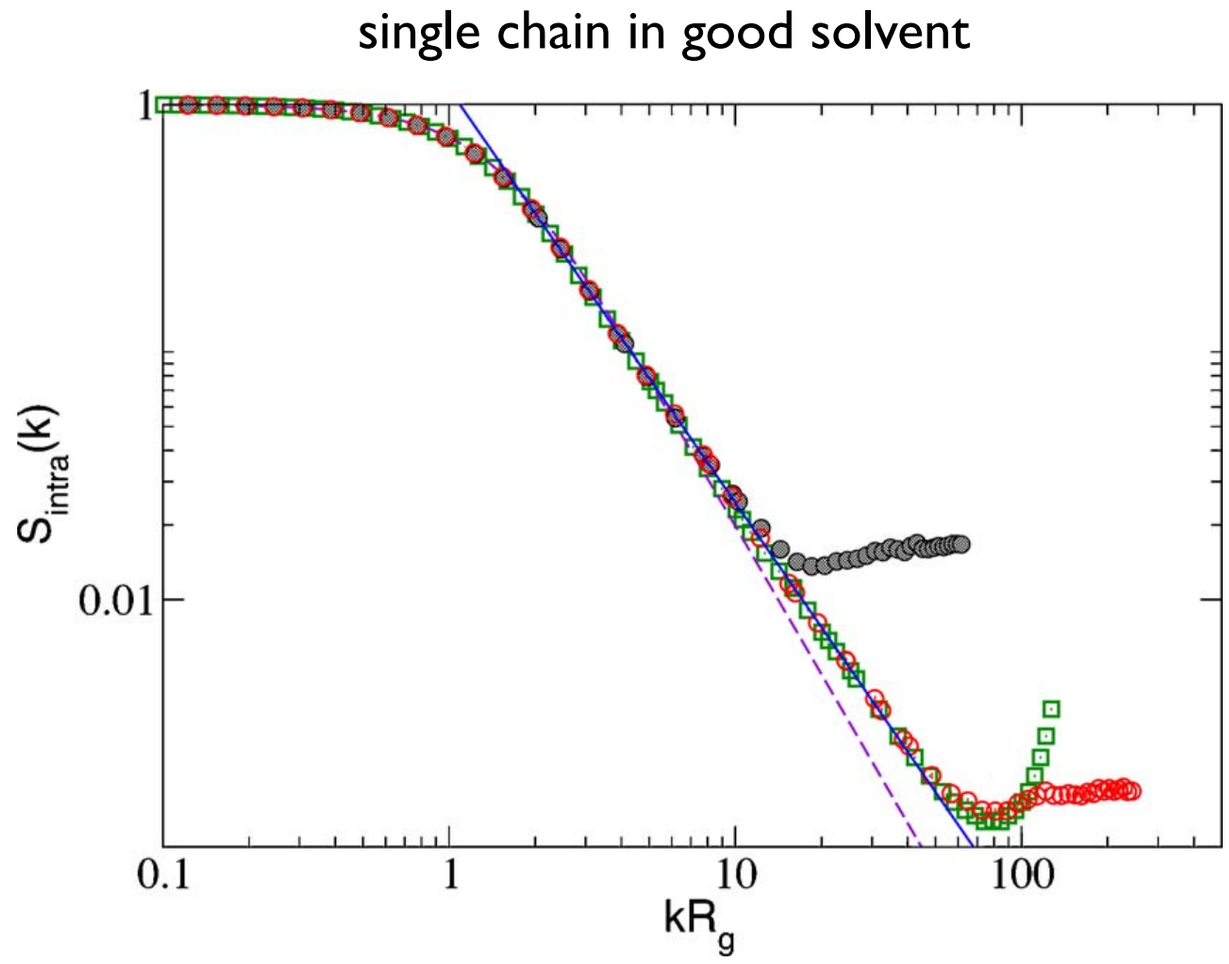

FIG. 2. (Color online) Intramolecular structure factor $S_{\text{intra}}(k)$ of a single SAW polymer vs kR_g on a log-log scale. Squares: MC data for an $L=1000$ SAW polymer: closed circles and open circles: MC data for $n=62$ and $n=602$ segment representations, respectively. Full line: scaling regime $1.15(kR_g)^{1/\nu}$, with $\nu \simeq 0.5988$; dashed line: Debye structure factor for a Gaussian chain.

Effective segment representation

up to 500 chains of given length N with different resolutions (*n* blobs)

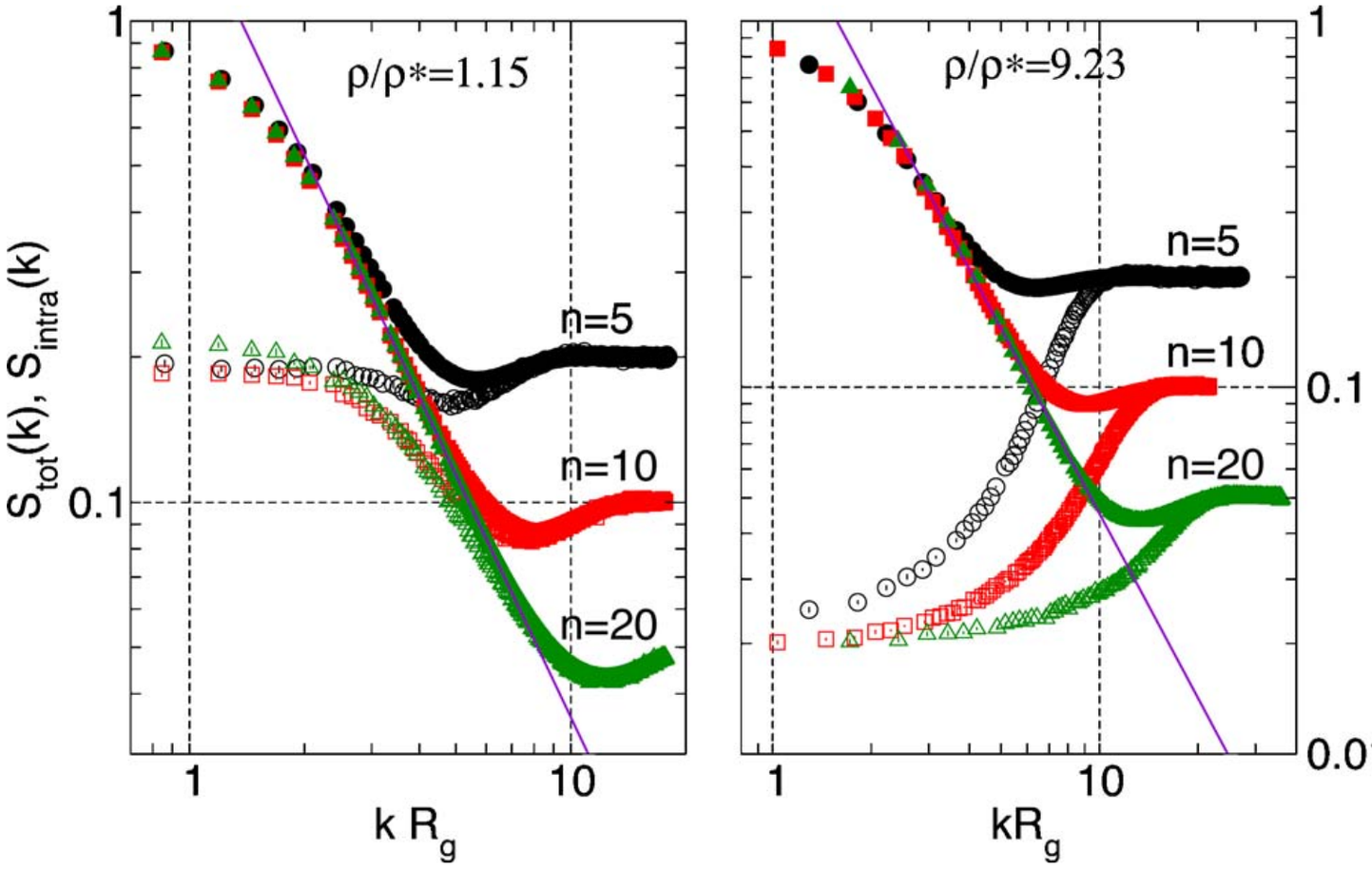

FIG. 3. (Color online) Total (closed symbols) and intramolecular (open symbols) structure factors vs kR_g from MC simulations of $n=5$ (circles), $n=10$ (squares), and $n=20$ (triangles) segment representations of SAW polymers at $\rho/\rho^*=1.15$ (left frame) and 9.23 (right frame). The straight lines correspond to the scaling regime as in Fig. 2.

Agreement among different resolution is expected for $kr_g < 1$ ($kR_g \sim n^{\nu}$)
At r~9 the minimum number of blobs expected is 18

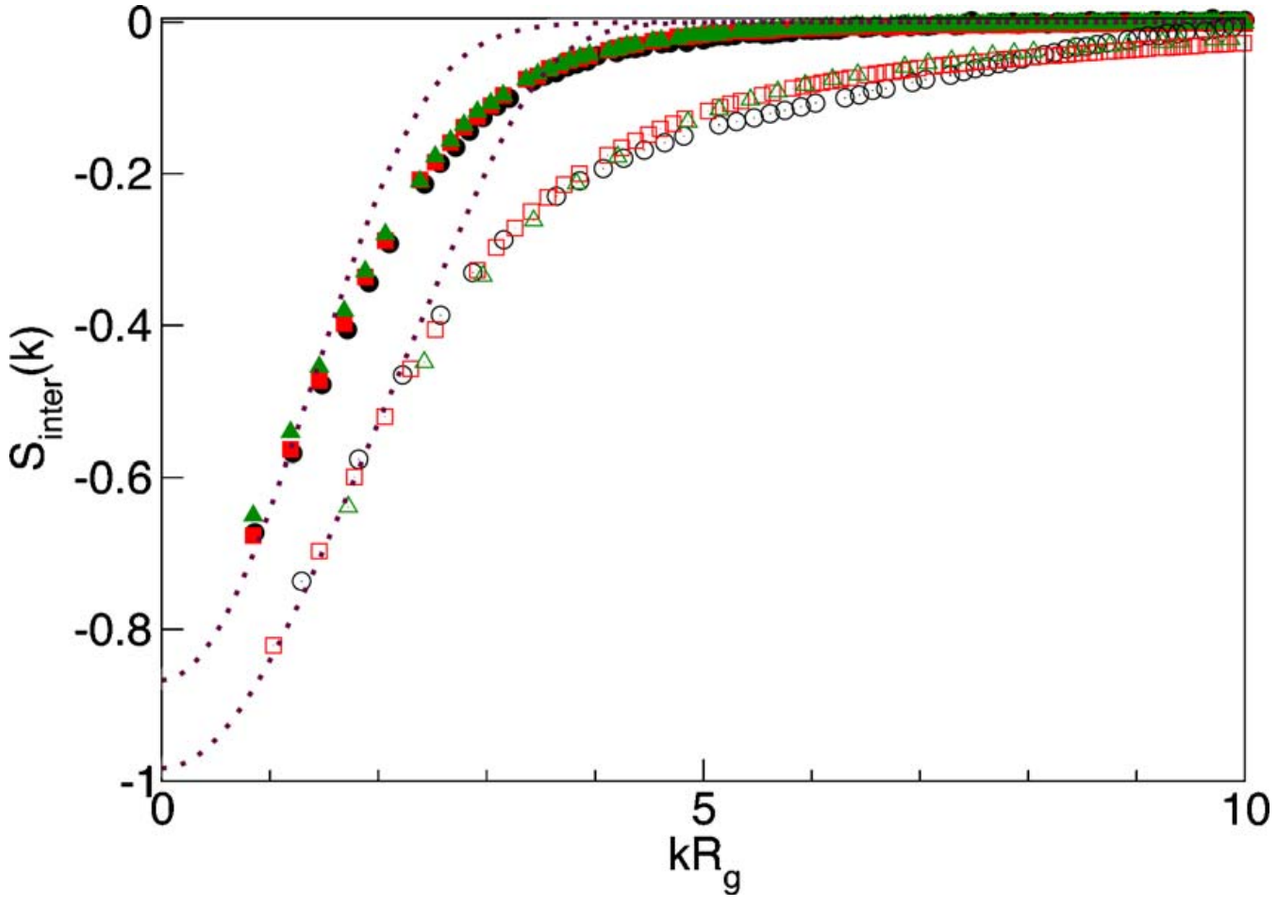

FIG. 4. (Color online) Intermolecular structure factor from MC simulation of $n=5$ (circles), 10 (squares), and 20 (triangles) segment representations of SAW polymers at densities $\rho/\rho^*=1.15$ (closed symbols) and 9.23 (open symbols) vs kR_g. The dashed curves are predictions of the RPA expression [Eq. (5)], using the intramolecular form factor (for $n=10$). The RPA is seen to be accurate for $kR_g \lesssim 2.5$, but to underestimate short-range correlations ($kR_g \gtrsim 2.5$).

$$\rho k_B T \chi_T = 1 + s_{\alpha\beta}(k \to 0)$$

At small k all $s_{ab}(k)$ become equal and we can estimate the compressibility from $S_{inter}(k)$ and from there the osmotic pressure

Agreement with the scaling law for the osmotic pressure is observed except at the higher density (9.2)

A-B diblock copolymer solutions

Styrene-Isoprene in DEP/DBP

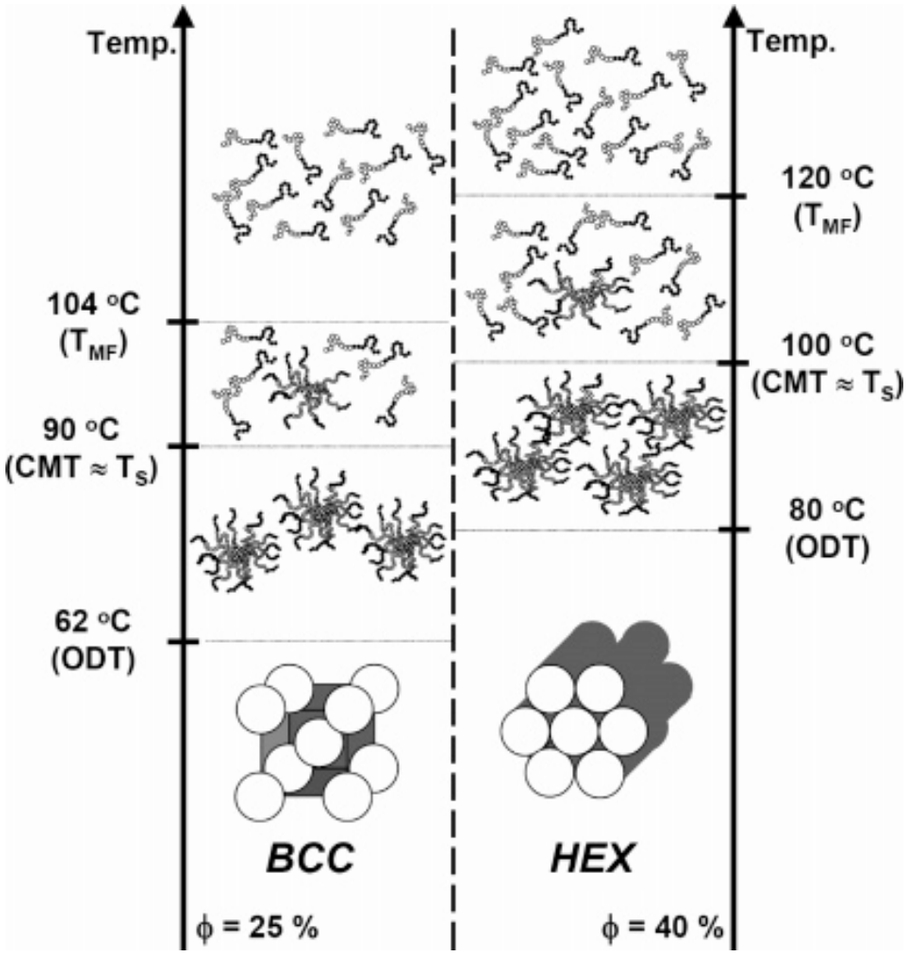

Figure 12. Phase behavior for 25% S*d*I(15−14) in DEP/DBP (75/25 vol %) and 40% S*d*I(15−14) in DEP/DBP (75/25 vol %). Bcc and HEX denote the body-centered cubic and the hexagonal cylinder, respectively, and ODT, cmt, T_S, and T_{MF} for the two solutions are shown. A schematic illustrating the regions of the micelles in long-range order, the disordered micelles along with associated transitions is also given.

Park et al. Macromolecules **38**, 2449 (2005)

Styrene-Isoprene DEP

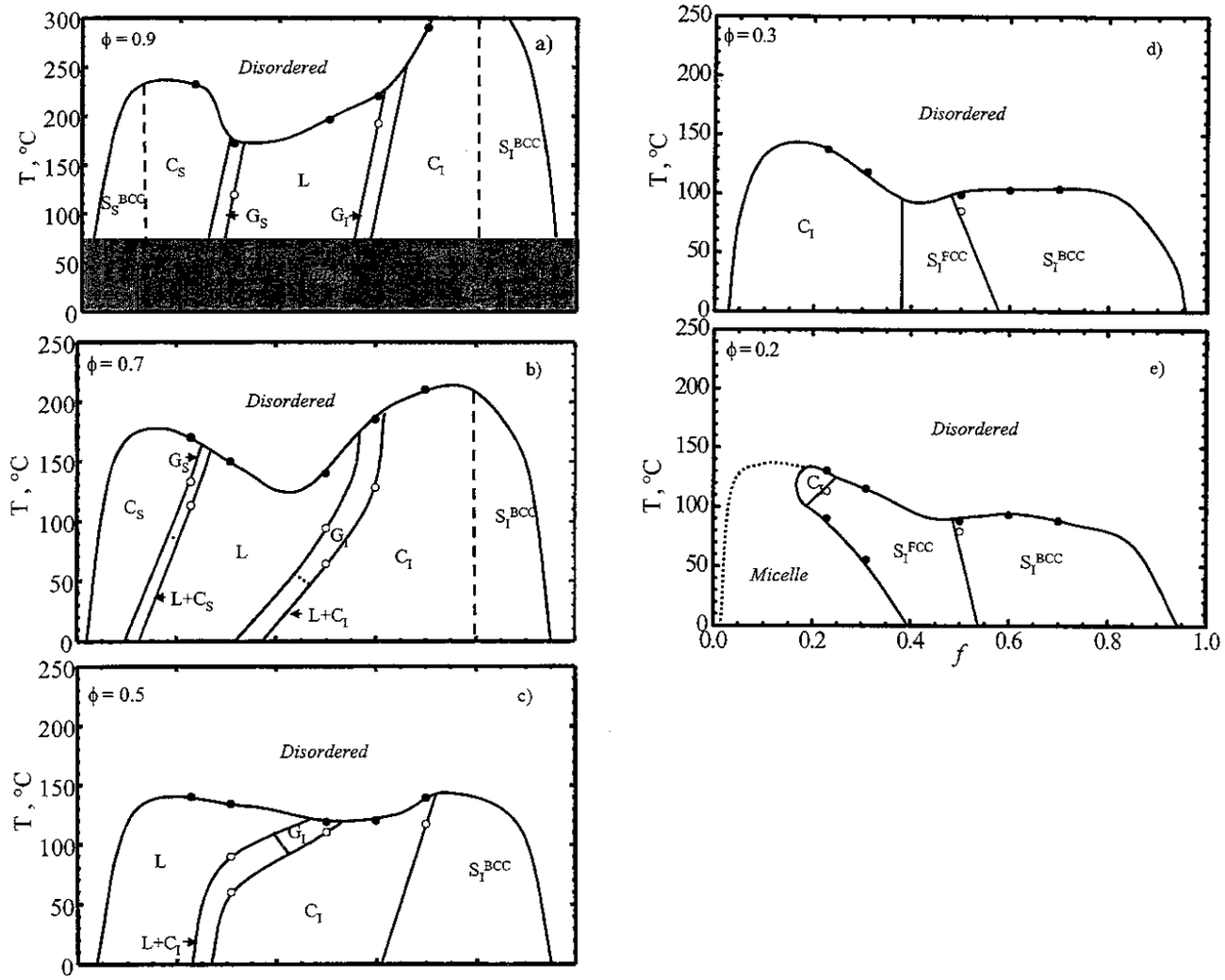

Varying concentration: $0.9 \geq \phi \geq 0.2$

Lodge et al., Macromolecules **35**, 4707 (2002)

Coarse Graining Strategy

1. **Full monomer description**:
   a. linear chain models on a cubic lattice
   b. implicit solvent represented by the monomer-monomer interactions
   c. Monte Carlo evaluation of chain properties

2. **First step of coarse graining**
   a. group a number of monomers around their centre of mass and represent that part of the chain by an effective monomer (blobs) with renormalized interactions
   b. the interaction between effective monomers are derived "ab-initio" from liquid state theory (HNC, RISM)
   c. Monte Carlo simulation of the effective chains system

3. **Second step of coarse graining**
   a. if spontaneous formation of aggregates is observed at the previous level of coarse graining, reduce each aggregate to its centre of mass.
   b. the interactions are again obtained by inverting the liquid structure

Di-block copolymers

- N linear chains of $M=M_A+M_B$ physical monomers on a cubic lattice.
- Athermal ISS model: A-A ideal, A-B and B-B self-avoiding.
- For $M\sim10^3$ and $N\sim10^2$ (chains per aggregate) each aggregate would have 10^5 monomers.
- Coarse graining: from linear chains to dumbbells
  - represent all monomers of each block by their centre of mass
  - potentials are obtained by inverting the CM-CM pair distribution functions generated in a full monomer simulation of two chains of $M_A=M_B=500$ monomers
  - approximation: zero density potentials are used at finite density (reasonable approximation for homopolymers up to $\rho/\rho^* \sim 4$)

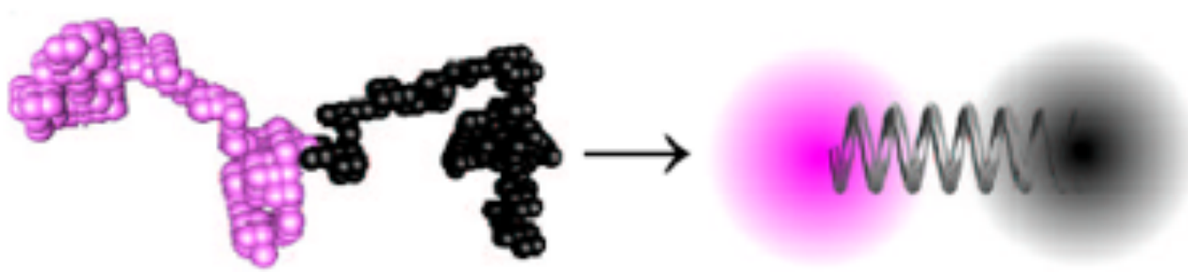

Zero density effective potentials between dumbbells

4308 The Journal of Chemical Physics, Vol. 62, No. 11, 1 June 1975

New type of cluster theory for molecular fluids: Interaction site cluster expansion*

Branka M. Ladanyi† and David Chandler‡

- solution of a four-body problem
- extension to finite density is not trivial

$$s_{AB}(r) = -k_B T \log[g_{AB}(r)]$$

$$\lim_{\rho\to 0} h_{AA}(\mathbf{r}) = f_{AA}(\mathbf{r}) + [1 + f_{AA}(\mathbf{r})] \left\{ \int d\mathbf{x} \, [f_{AB}(\mathbf{x}) s_{BA}(\mathbf{x}-\mathbf{r}) + s_{AB}(\mathbf{x}) f_{BA}(\mathbf{x}-\mathbf{r})] \right.$$
$$+ \int d\mathbf{x} \int d\mathbf{y} s_{AB}(\mathbf{x}) s_{BA}(\mathbf{y}-\mathbf{r}) \, [f_{BB}(\mathbf{x}-\mathbf{y}) + f_{AB}(\mathbf{y}) f_{BB}(\mathbf{x}-\mathbf{y}) + f_{BA}(\mathbf{x}-\mathbf{r}) f_{BB}(\mathbf{x}-\mathbf{y})$$
$$\left. + f_{AB}(\mathbf{y}) f_{BA}(\mathbf{x}-\mathbf{r}) + f_{AB}(\mathbf{y}) f_{BA}(\mathbf{x}-\mathbf{r}) f_{BB}(\mathbf{x}-\mathbf{y})] \right\} \quad (8)$$

$$\lim_{\rho\to 0} h_{AB}(\mathbf{r}) = f_{AB}(\mathbf{r}) + [1 + f_{AB}(\mathbf{r})] \left\{ \int d\mathbf{x} \, [f_{AA}(\mathbf{x}) s_{AB}(\mathbf{x}-\mathbf{r}) + s_{AB}(\mathbf{x}) f_{BB}(\mathbf{x}-\mathbf{r})] \right.$$
$$+ \int d\mathbf{x} \int d\mathbf{y} s_{AB}(\mathbf{x}) s_{AB}(\mathbf{y}-\mathbf{r}) \, [f_{BA}(\mathbf{x}-\mathbf{y}) + f_{AA}(\mathbf{y}) f_{BA}(\mathbf{x}-\mathbf{y}) + f_{BB}(\mathbf{x}-\mathbf{r}) f_{BA}(\mathbf{x}-\mathbf{y})$$
$$\left. + f_{AA}(\mathbf{y}) f_{BB}(\mathbf{x}-\mathbf{r}) + f_{AA}(\mathbf{y}) f_{BB}(\mathbf{x}-\mathbf{r}) f_{BA}(\mathbf{x}-\mathbf{y})] \right\}. \quad (9)$$

where $h_{\alpha\beta}(\mathbf{r}) = g_{\alpha\beta}(\mathbf{r}) - 1$ and the $f_{\alpha\beta}(\mathbf{r})$ are the Mayer functions

$$f_{\alpha\beta}(\mathbf{r}) = f_{\beta\alpha}(\mathbf{r}) = \exp[-\beta v_{\alpha\beta}(\mathbf{r})] - 1, \quad (10)$$

First coarse graining step

For diblock copolymer we used two different sets of potentials:

- from homopolymers simulations:
- from "diatomic molecule": RISM integral equation (Ladanyi Chandler, J. Chem. Phys. 1975)
- the intramolecular A-B interaction is extracted from the intrachain CM-CM pair correlation function $\phi_{\alpha\beta}(r) = -\log[g_{\alpha\beta}(r)]$

- Two sets of potentials are very close except for V_{AA}
- Potentials are repulsive and finite at R=0
- Interaction range ~ 2Rg
- AB and BB potentials are well represented by gaussians

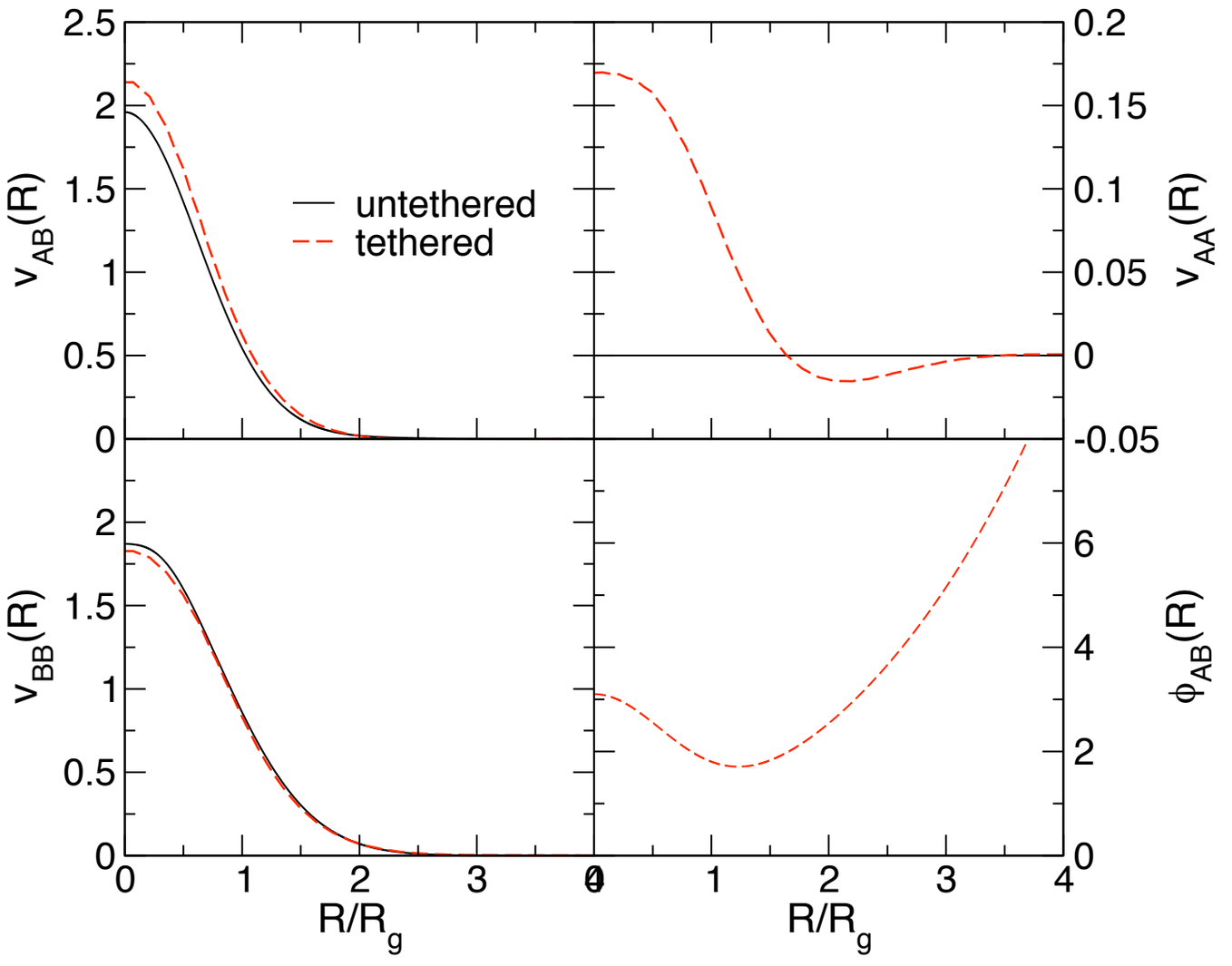

RPA prediction of clustering (B. Capone et al, JPCB **113**, 3629 (2009))

$$\underline{S}^{-1}(k) = \underline{S_0}^{-1}(k) + \rho\beta\underline{\hat{V}}(k)$$

$$S_{\alpha\beta}(k) = \frac{f_{\alpha\beta}(k,\rho)}{D_c(k,\rho)}$$

$$\underline{S_0}(k) = \begin{pmatrix} 1 & \hat{s}_{AB}(k) \\ \hat{s}_{AB}(k) & 1 \end{pmatrix}$$

$$D_c(k,\rho) = 1 + \rho\beta[\hat{v}_{AA}(k) + \hat{v}_{BB}(k) - 2\hat{s}_{AB}(k)\hat{v}_{AB}(k)] + \rho^2\beta^2[\hat{v}_{AA}(k)\hat{v}_{BB}(k) - \hat{v}^2_{AB}(k)][1 - \hat{s}^2_{AB}(k)] \quad (10)$$

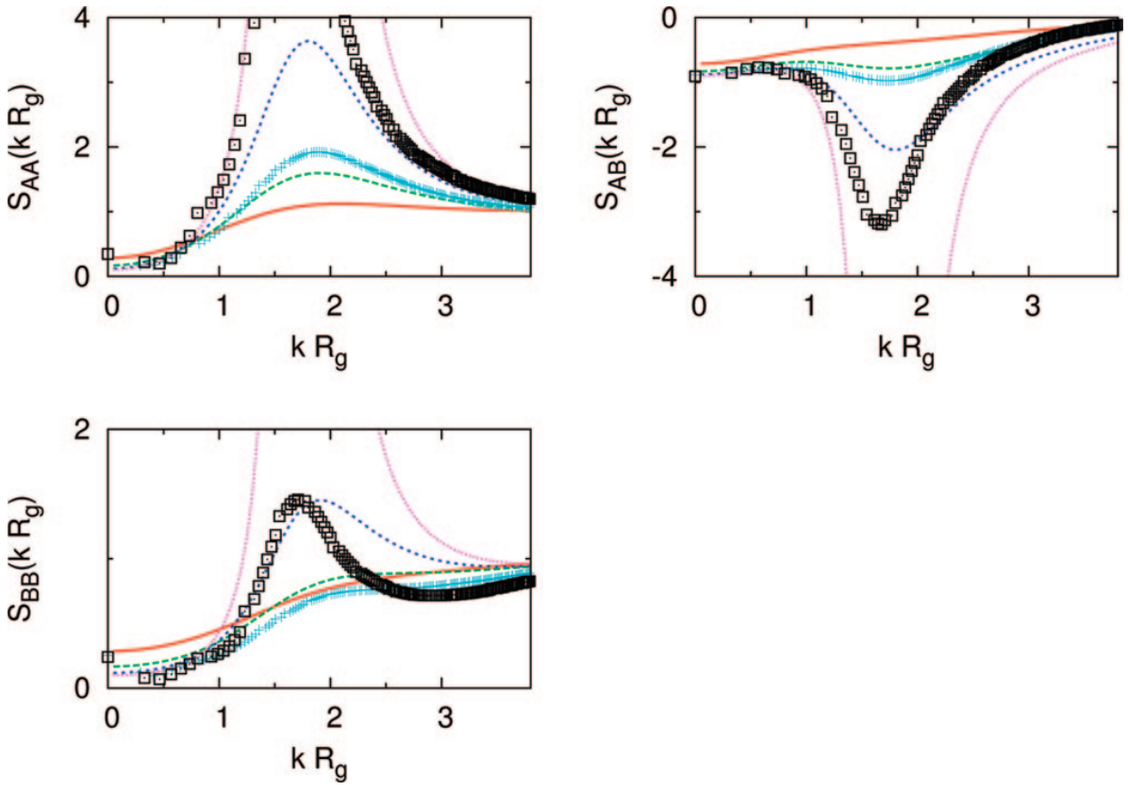

Figure 3. RPA predictions (eqs 9 and 10) for the partial structure factors $S_{\alpha\beta}$ as functions of the reduced wavenumbers kR_g for AB diblock copolymers with $f = 0.6$ in the soft dumbbell representation. The full curve, dashes, large dots, and small dots are for reduced densities $\rho/\rho^* = 0.5$, 1, 1.5, and 1.85 respectively, while the crosses and squares are MC data for $\rho/\rho^* = 2.5$ and 3.

TABLE 2: Critical Density ρ_c at which the RPA Structure Factors Diverge, Using the Diblock Copolymer Effective Potential Parameters (Diblock Copolymer Potentials DBP) and the Binary Mixture Effective Potential Parameters, Combined with the Diblock Tethering Potential (Binary Mixture Potentials BMP)[a]

f	DBP	BMP	cmc
1/5	25.0	12.57	$\rho/\rho^* > 7$
2/5	4.97	4.27	$4 < \rho/\rho^* < 4.5$
1/2	2.83	2.44	$3 < \rho/\rho^* < 3.5$
3/5	2.02	1.85	$2.5 < \rho/\rho^* < 3.$
4/5	1.65	1.13	$2 < \rho/\rho^* < 2.5$

[a] The MC estimates of the cmc are given in the right-hand column.

Self-assembling of effective copolymers

(C. Perleoni et al., PRL 96 128302 (2006))

- Systems of 10^4 dumbbells at constant density in the range $3 \leq \rho/\rho^* \leq 10$
- Spontaneous self-assembling in spherical micelles with A specie in the core and B specie in the corona at $\rho/\rho^* \sim 4$

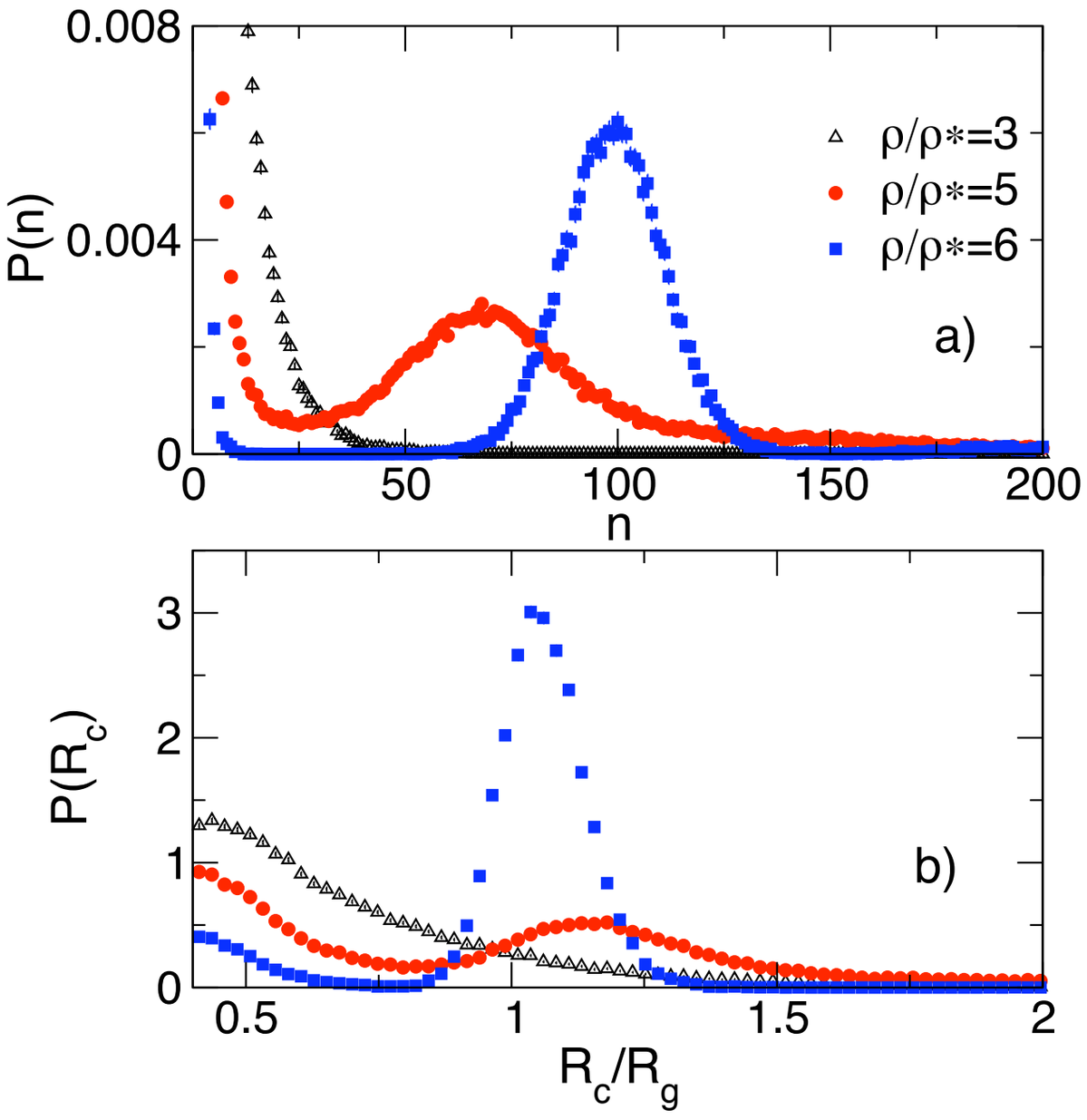

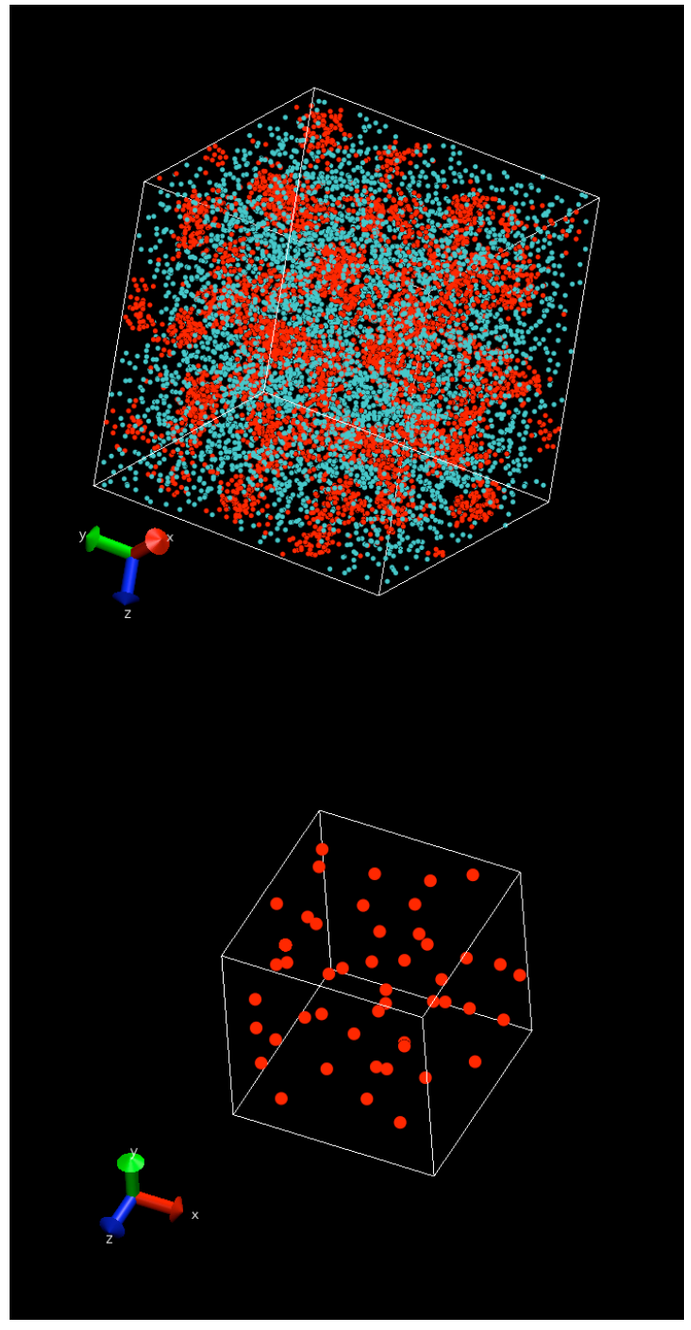

Critical Micelle Concentration (CMC)

• CMC is defined as the density at which $\sum_{i=1}^{n_0} iP(i) = \sum_{j=n_0+1}^{N} jP(j)$ where n_0 is the size at which P(n) has a minimum

• thermodynamic signature of the microphase separation associated with micellization

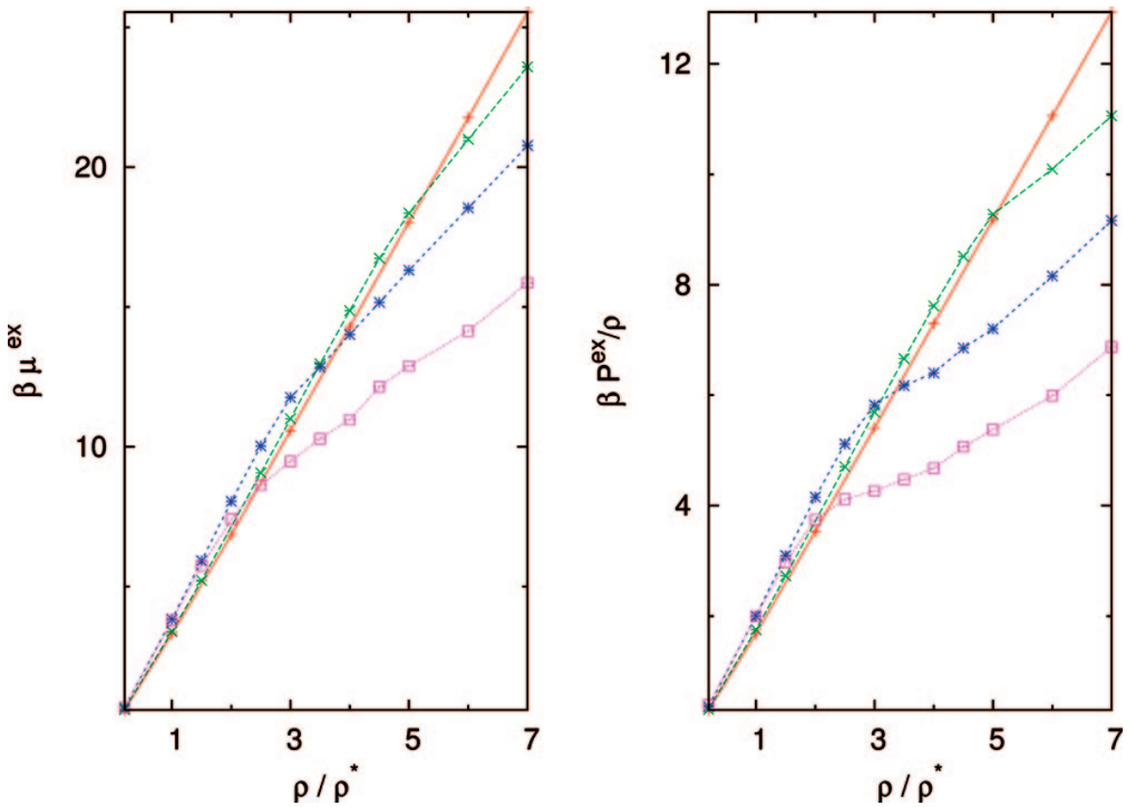

Figure 10. Reduced excess (nonideal) chemical potential $\beta\mu^{ex}$ (left frame), and osmotic equation of state $\beta P^{ex}/\rho$ (right frame) versus reduced copolymer density ρ/ρ^* for $f = 0.2$ (pluses), 0.4 (crosses), 0.6 (stars), and 0.8 (squares). The corresponding slopes of the RPA prediction (eq 15) are $\zeta = 3.48$ for $f = 0.2$, 4.20 for $f = 0.4$, 4.68 for $f = 0.6$, and 4.7 for $f = 0.8$.

$$\beta\mu_{ex}^{RPA} = \zeta\frac{\rho}{\rho^*}$$

RPA:

$$\frac{\beta P}{\rho} = 1 + \frac{\zeta}{2}\frac{\rho}{\rho^*}$$

Micelles crystallization at higher density

• At $\rho/\rho^* = 6$ the system of micelles with f=0.5 undergoes a spontaneous crystallization into an ordered structure with defects

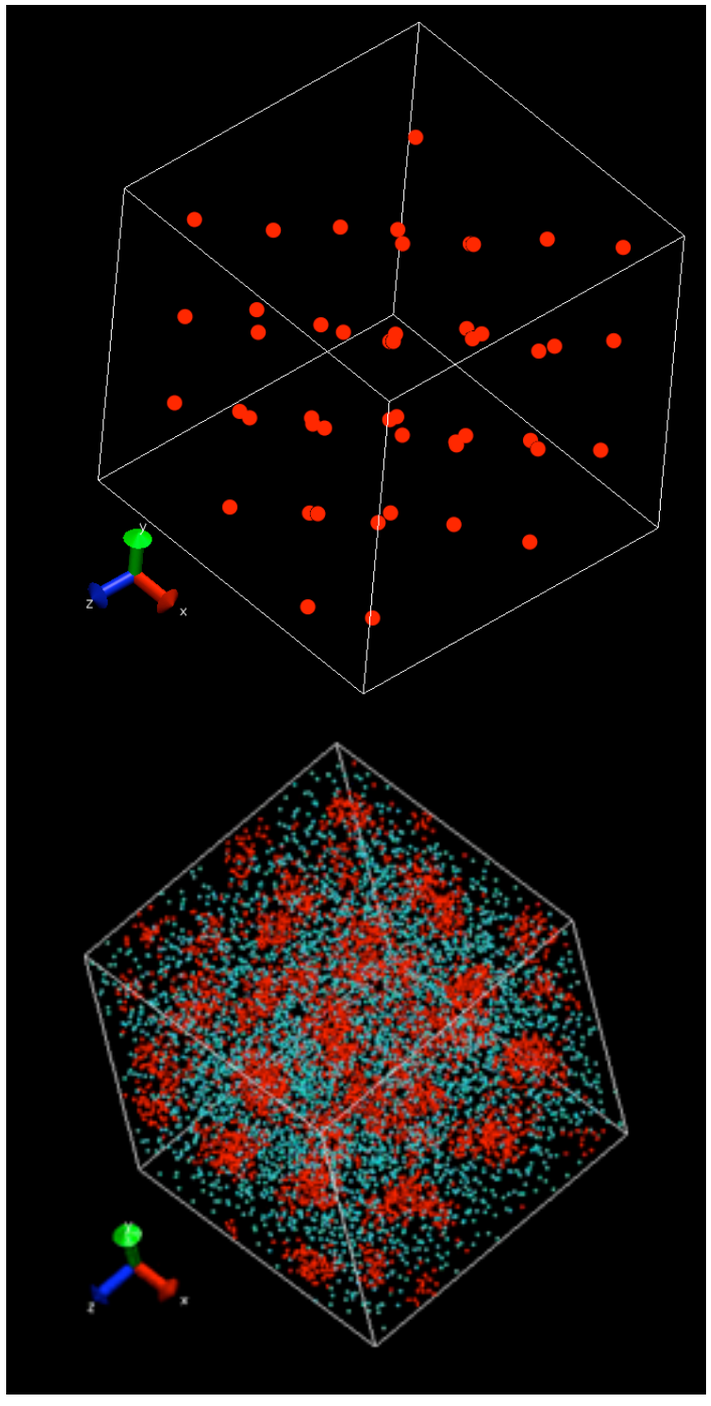

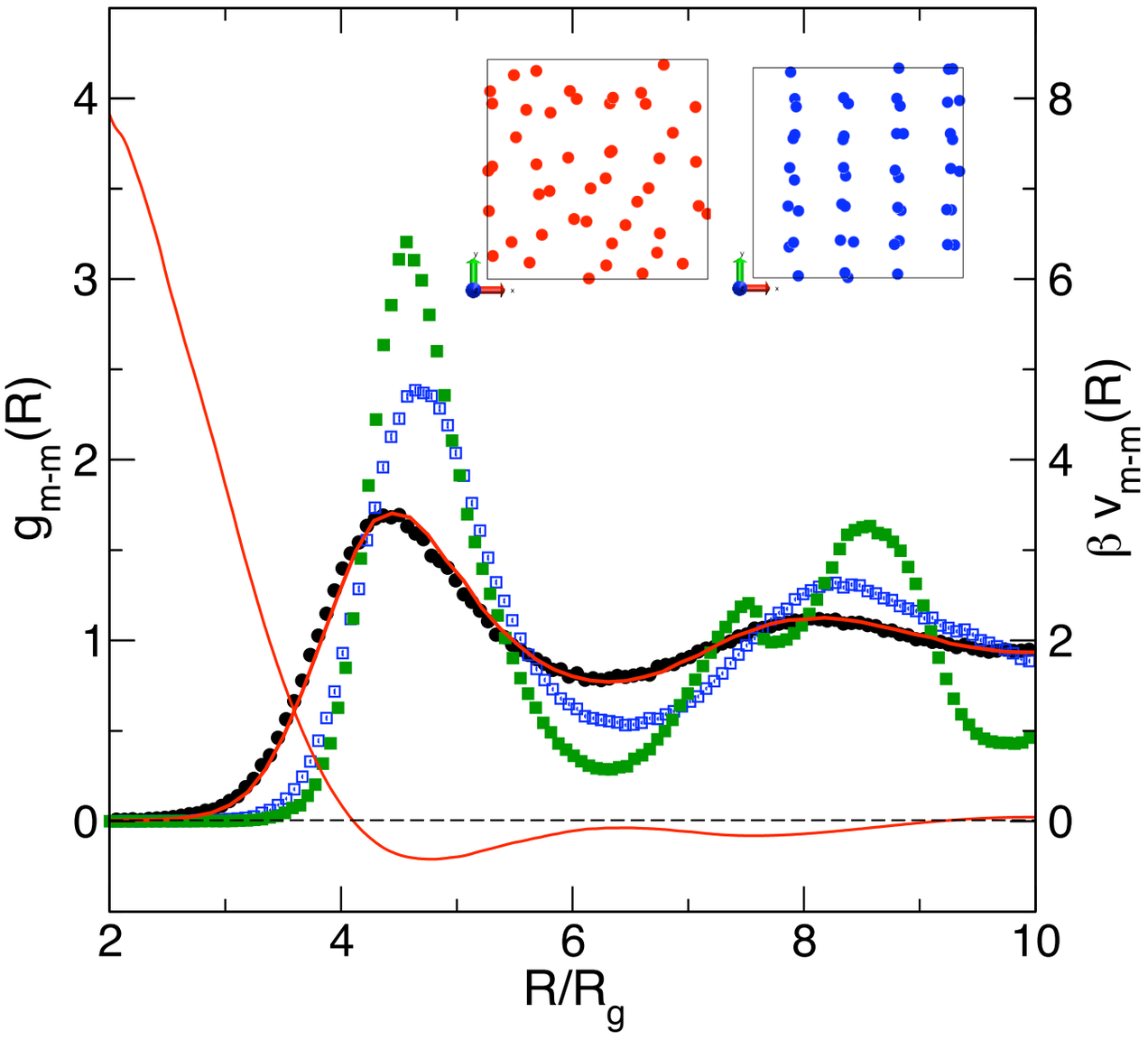

Pair correlation functions between the centers of mass of aggregates for increasing density.
f=0.5

Second coarse graining step

Reduce each aggregate to a point particle located at its center of mass. The interaction potential is extracted by inverting $g_{mm}(R)$ within the HNC approximation

$$\beta v_m(R) = g_{mm}(R) - 1 - c_{mm}(R) - \log[g_{mm}(R)]$$

Special care is needed here because of the partial knowledge of g(r) at large R.

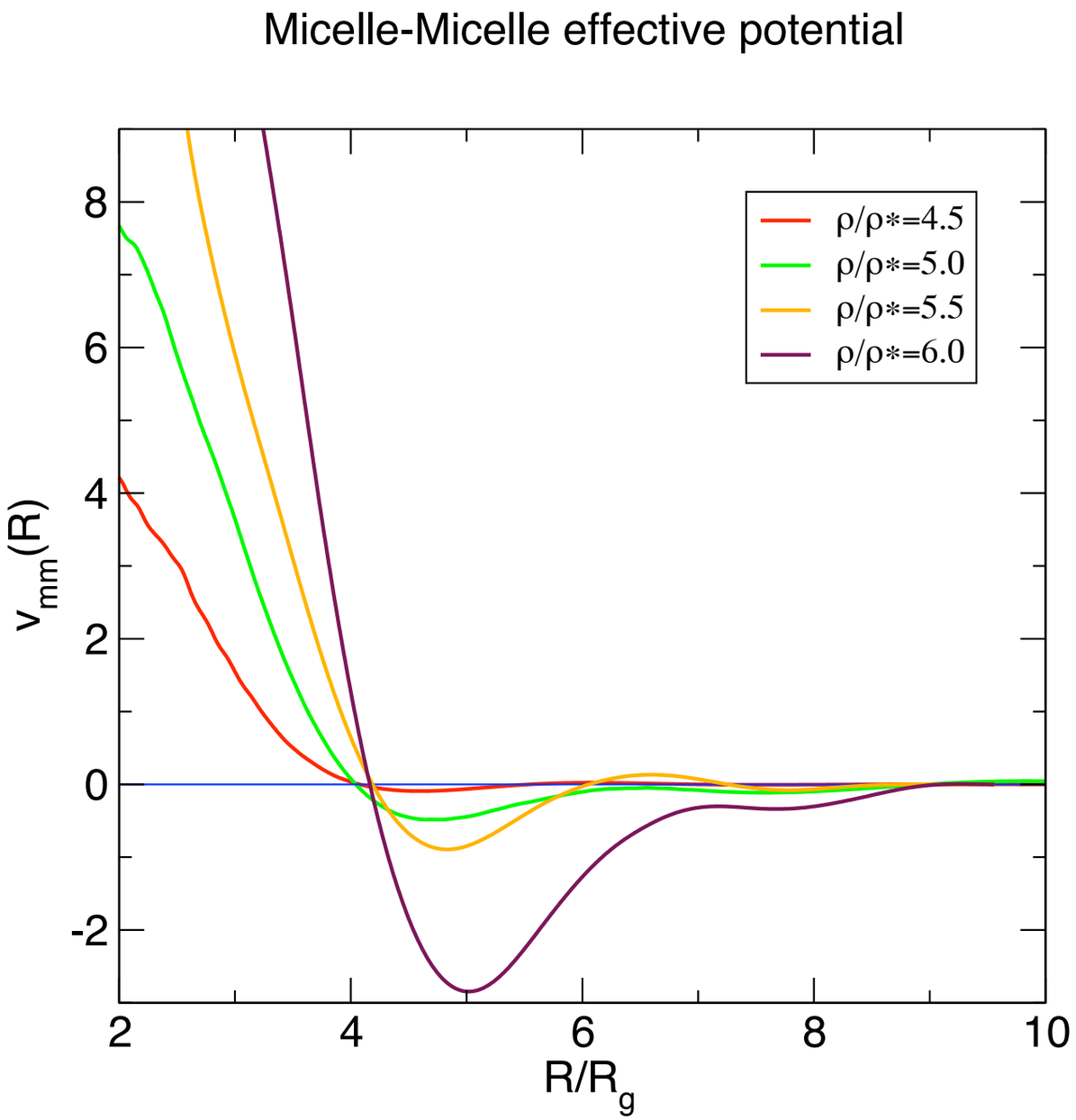

- The density dependent potential develops an attractive part at intermediate distances
- The effect is purely entropic!!
- The stiffness of the potential rapidly increases with density

Second coarse graining step

Molecular Physics
Vol. 107, Nos. 4–6, 20 February–20 March 2009, 535–548

INVITED ARTICLE

Crystal stability of diblock copolymer micelles in solution

John Jairo Molina[ab]*, Carlo Pierleoni[c], Barbara Capone[d],
Jean-Pierre Hansen[ad] and Igor Saulo Santos de Oliveira[be]

The effective potentials provide an accurate structure for all f and all densities

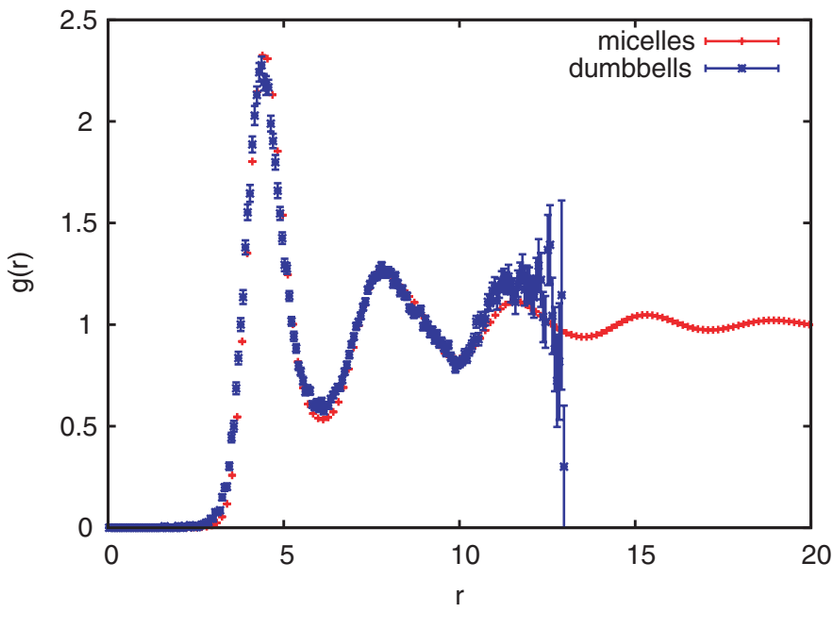

Figure 1. (Colour online). Micelle–micelle pair distribution function $g(r)$ calculated from dumbbell-level and micelle level MC simulations, for $f=0.4$ and $\rho/\rho*=6$. The former data have large statistical uncertainties for the range of micelle–micelle distances $L/2 < r < L3^{1/2}/2$, where the upper limit is the largest distance accessible in a cubic simulation box.

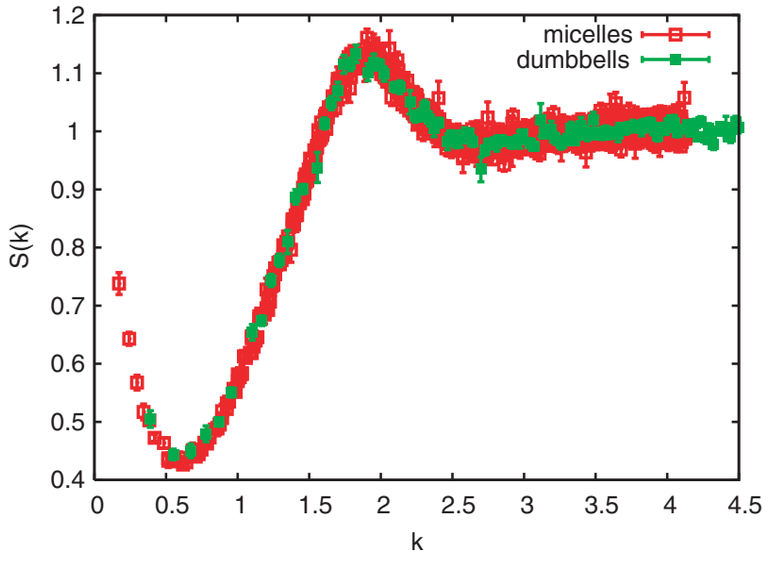

Figure 5. (Colour online). Micelle–micelle structure factors at $f=0.4$ and $\rho/\rho*=5$. Comparison between the full dumbbell representation (solid squares) and the effective micelle model (open squares).

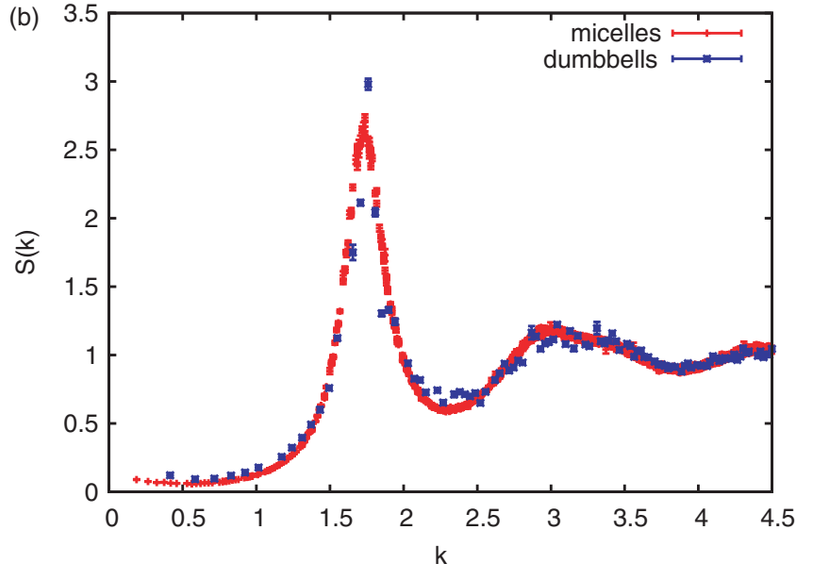

Figure 4. (Colour online). (a) MC-generated $g(r)$ for $f=0.4$, $\rho/\rho*=6$, starting from a perfect FCC configuration of the micelles. The vertical segments indicate the positions of the first shells of nearest neighbours in the initial FCC lattice, and their height indicates the corresponding coordination number (right-hand scale). (b) Corresponding structure factors $S(k)$ (pluses). The structure factor calculated directly from dumbbell level MC simulations is shown as crosses.

Crystal structure stability at high density

- At $\rho/\rho^* = 6$ the effective-micelles system is able to sustain crystal structures
- We have studied the relative stability of BCC, FCC and A15 structures

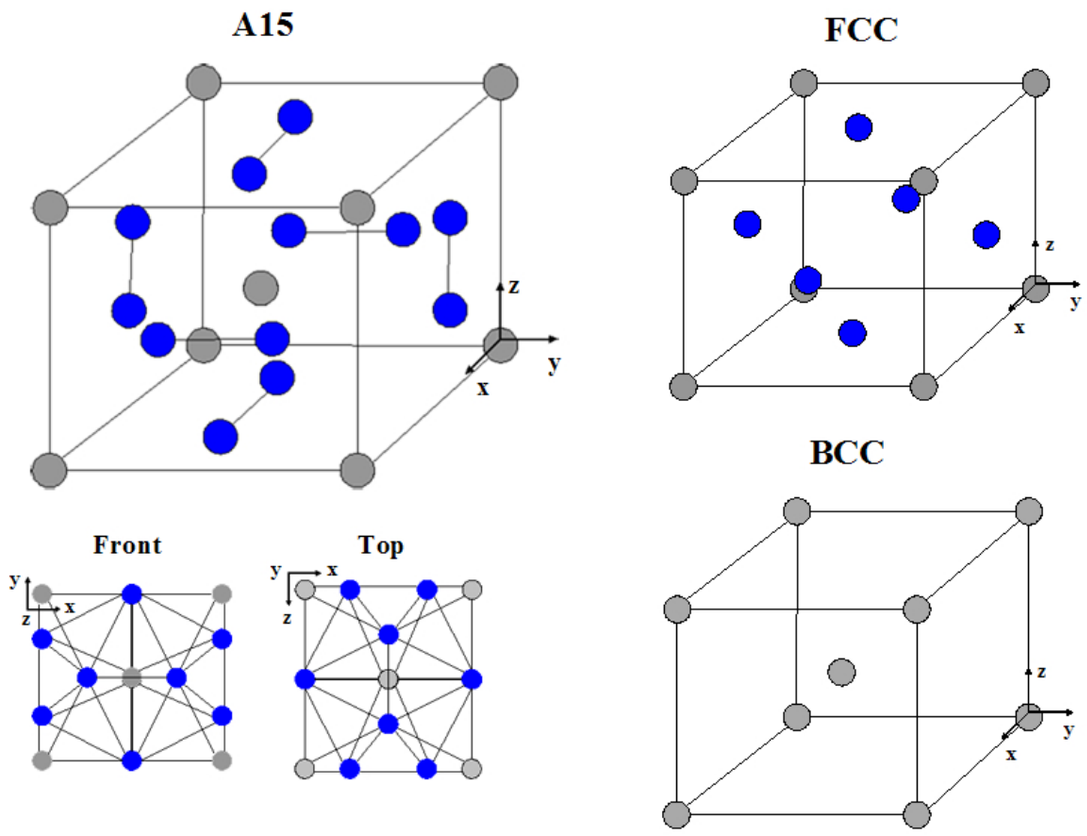

Figure 4.8: A15 unit cell and views (top and front), FCC and BCC unit cells.

- A15 minimize the ratio area/volume of the Voronoi cells (Weaire and Phelan, Phil.Mag. Lett, **69**, 107 (1994))
- A15 is not a close-packed structure, it has been predicted in micelles of dentritic polymers (Ziherl and Kamien, Phys. Rev. Letts. **85**, 3528 (2000))

Crystal structure stability at high density

- At $\rho/\rho^* = 5.5$ the system rapidly melts for all initial conditions
- At $\rho/\rho^* = 6$ the three structures are stable

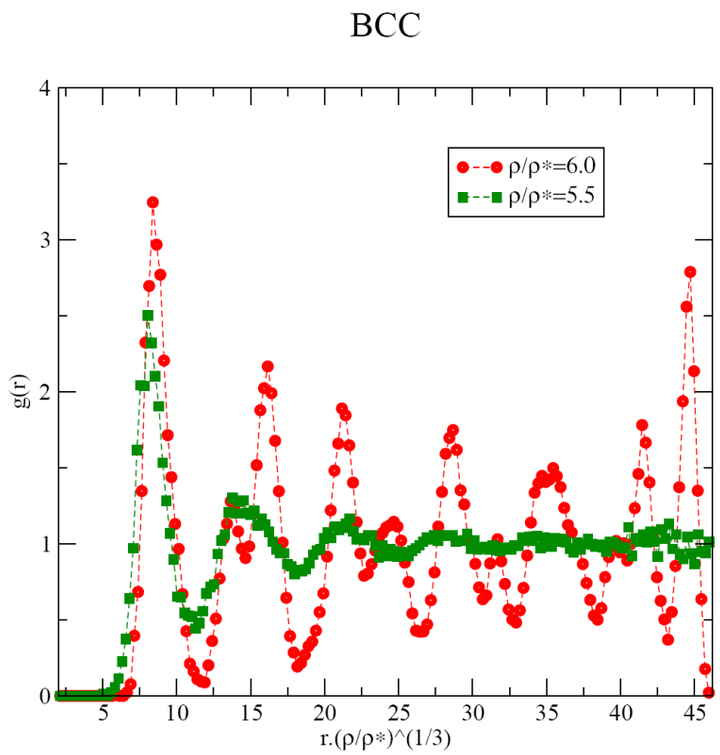

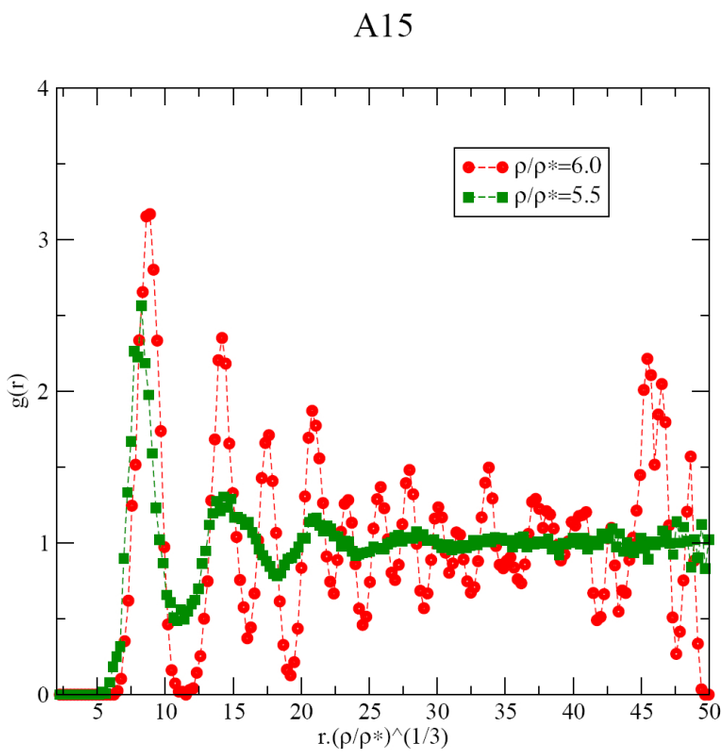

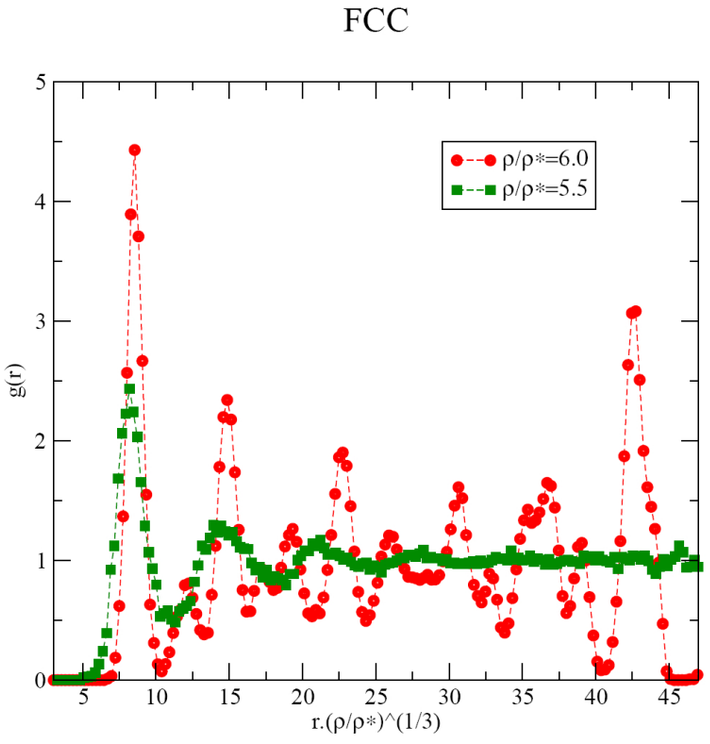

f=0.5

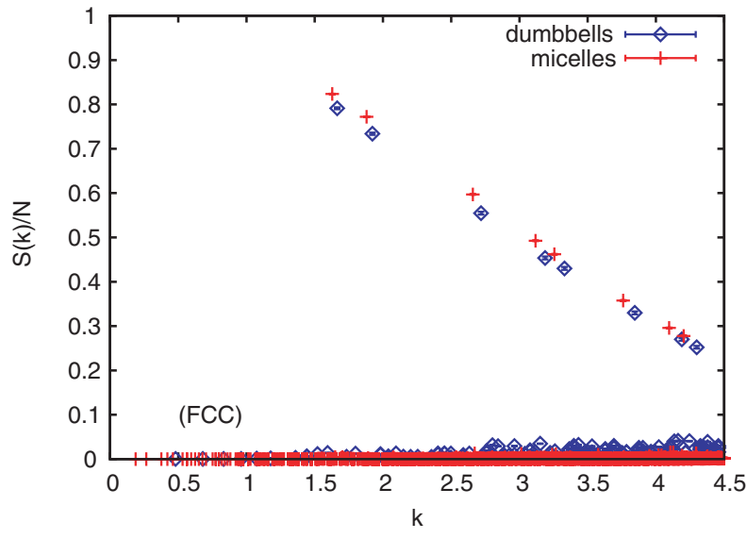

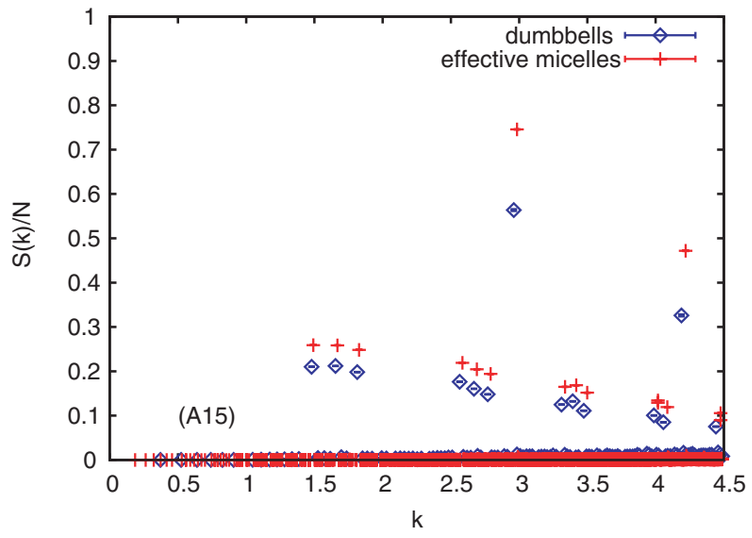

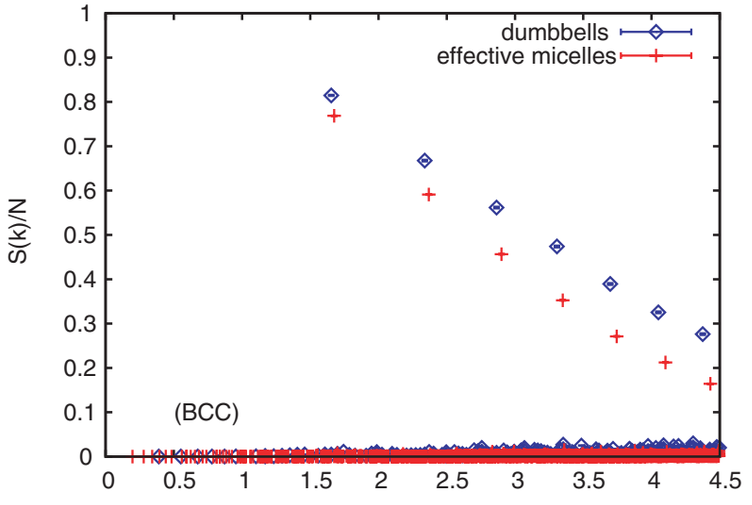

Free energy calculations for the effective micelles model

system	BCC	FCC	A15	LIQUID
$f = 0.4, \rho/\rho^* = 7$	-20.4343(4)	-20.8418(1)	-21.1049(1)	-----
$f = 0.5, \rho/\rho^* = 6$	-13.419(1)	-13.508(1)	-13.554(1)	-12.843(1)
$f = 0.6, \rho/\rho^* = 4$	-----	-1.1222(1)	-1.1215(1)	-1.076(1)

Ladd-Frenkel method in the crystal phases
Coupling constant integration in the liquid phase

Conclusions

• We have developed a consistent and efficient strategy for the coarse graining of diblock copolymer solutions.

• The coarse-grained ISS dumbbells model exhibits the spontaneous self-assembling of the polymers into spherical micelles and the micelle crystallization for increasing density in qualitative agreement with experiments

• Signature of the micellization (CMC) are observed in thermodynamic properties and can be anticipated within the RPA, with good agreement with simulations

•Above the CMC, micelles of dumbbells can be safely replaced by point particles with suitably extracted pair potentials, providing an effective micelles model to study the relative stability of various phases

•By free energy methods we have found the A15 structure to be the most stable structure among our three candidates, while diamond structure, observed in star polymers, is always dynamically unstable.

Open issues

• Our coarse graining strategy from full monomer to dumbbells is based on the use of potentials extracted at zero density. The use of such potentials for concentrated solutions is an untested approximation. Needs for a multi-blob approach (work in progress by B. Capone)

• In going from dumbbells micelles to effective point particles important aspects of the original systems, such as polydispersity of the aggregates, dynamical fluctuations of the number of aggregates in the systems, chemical equilibrium between free molecules and aggregates, are lost.

• Although predictions from the effective micelle model are in qualitative agreement with results for the dumbbells model, a quantitative validation of this further coarse-graining step is still missing.

• Calculation of crystal free energies for dumbbells micelles are in progress (G. D'Adamo) by using a recently developed method:

PRL **99,** 235702 (2007) PHYSICAL REVIEW LETTERS week ending 7 DECEMBER 2007

Phase Coexistence of Cluster Crystals: Beyond the Gibbs Phase Rule

Bianca M. Mladek,[1] Patrick Charbonneau,[2] and Daan Frenkel[2,*]

Aknowledgements

- J. P. Hansen, University of Cambridge, UK
- V. Krakoviak, ENS-Lyon, France
- C.I. Addison, University of Cambridge, UK
- B. Capone, University of Cambridge, UK
- I.S. Santos de Oliveira, University of Rome “La Sapienza”, Italy
- J.M. Molina, University of Rome “La Sapienza”, Italy
- G. D’Adamo, University of L’Aquila, Italy.